Am J Physiol Heart Circ Physiol 312: H1176–H1184, 2017.
First published March 31, 2017; doi:10.1152/ajpheart.00097.2017.

RESEARCH ARTICLE | *Vascular Biology and Microcirculation*

Reduced membrane cholesterol limits pulmonary endothelial Ca^{2+} entry after chronic hypoxia

Bojun Zhang, Jay S. Naik, Nikki L. Jernigan, Benjimen R. Walker, and Thomas C. Resta

Vascular Physiology Group, Department of Cell Biology and Physiology, University of New Mexico Health Sciences Center, Albuquerque, New Mexico

Submitted 13 February 2017; accepted in final form 24 March 2017

Zhang B, Naik JS, Jernigan NL, Walker BR, Resta TC. Reduced membrane cholesterol limits pulmonary endothelial Ca^{2+} entry after chronic hypoxia. *Am J Physiol Heart Circ Physiol* 312: H1176–H1184, 2017. First published March 31, 2017; doi: 10.1152/ajpheart.00097.2017.—Chronic hypoxia (CH)-induced pulmonary hypertension is associated with diminished production of endothelium-derived Ca^{2+}-dependent vasodilators such as nitric oxide. Interestingly, ATP-induced endothelial Ca^{2+} entry as well as membrane cholesterol (Chol) are decreased in pulmonary arteries from CH rats (4 wk, barometric pressure = 380 Torr) compared with normoxic controls. Store-operated Ca^{2+} entry (SOCE) and depolarization-induced Ca^{2+} entry are major components of the response to ATP and are similarly decreased after CH. We hypothesized that membrane Chol facilitates both SOCE and depolarization-induced pulmonary endothelial Ca^{2+} entry and that CH attenuates these responses by decreasing membrane Chol. To test these hypotheses, we administered Chol or epicholesterol (Epichol) to acutely isolated pulmonary arterial endothelial cells (PAECs) from control and CH rats to either supplement or replace native Chol, respectively. The efficacy of membrane Chol manipulation was confirmed by filipin staining. Epichol greatly reduced ATP-induced Ca^{2+} influx in PAECs from control rats. Whereas Epichol similarly blunted endothelial SOCE in PAECs from both groups, Chol supplementation restored diminished SOCE in PAECs from CH rats while having no effect in controls. Similar effects of Chol manipulation on PAEC Ca^{2+} influx were observed in response to a depolarizing stimulus of KCl. Furthermore, KCl-induced Ca^{2+} entry was inhibited by the T-type Ca^{2+} channel antagonist mibefradil but not the L-type Ca^{2+} channel inhibitor diltiazem. We conclude that PAEC membrane Chol is required for ATP-induced Ca^{2+} entry and its two components, SOCE and depolarization-induced Ca^{2+} entry, and that reduced Ca^{2+} entry after CH may be due to loss of this key regulator.

NEW & NOTEWORTHY This research is the first to examine the direct role of membrane cholesterol in regulating pulmonary endothelial agonist-induced Ca^{2+} entry and its components. The results provide a potential mechanism by which chronic hypoxia impairs pulmonary endothelial Ca^{2+} influx, which may contribute to pulmonary hypertension.

pulmonary hypertension; T-type calcium channels; ATP; store-operated Ca^{2+} entry; depolarization-induced Ca^{2+} entry

PULMONARY VASCULAR DYSFUNCTION resulting from chronic hypoxia (CH) leads to increased vascular resistance and pulmonary hypertension in patients with chronic lower respiratory diseases and sleep apnea and in residents at high altitude. Vasoconstriction and vascular remodeling associated with dysregulation of endothelium-derived mediators are the major components of elevated vascular resistance in CH-induced pulmonary hypertension. Production of many endothelium-dependent vasoactive substances as well as regulation of membrane potential are largely a function of pulmonary endothelial intracellular Ca^{2+} concentration ($[Ca^{2+}]_i$) levels. For example, $[Ca^{2+}]_i$ is a key regulatory factor in the activity of endothelial nitric oxide (NO) synthase (8, 16, 34, 41), phospholipase A_2 (PLA_2) (53, 54), and the small- and intermediate-conductance Ca^{2+}-activated K^+ channels (SK_{Ca} and IK_{Ca}, respectively) that are responsible for endothelial cell hyperpolarization upon activation by agonists (21, 29). Diminished pulmonary endothelial $[Ca^{2+}]_i$ may limit production of endothelium-derived vasodilators and antimitogenic substances, including NO, prostacyclin, and endothelium-derived hyperpolarizing factors. Although endothelial dysfunction and associated decreases in pulmonary artery endothelial $[Ca^{2+}]_i$ and endothelium-derived NO (32, 37–39) may be contributing factors to the development of CH-induced pulmonary hypertension, the mechanisms by which endothelial $[Ca^{2+}]_i$ is reduced after CH are incompletely understood.

Our previous studies have demonstrated that both basal $[Ca^{2+}]_i$ and agonist-induced Ca^{2+} influx are lower in pulmonary artery endothelial cells (PAECs) from CH rats compared with those of control rats (37, 38). CH similarly inhibits store-operated Ca^{2+} entry (SOCE) and depolarization-induced Ca^{2+} influx through T-type voltage-gated Ca^{2+} channels (VGCCs), which are major components of agonist-induced Ca^{2+} entry in isolated PAECs (37, 39). Furthermore, agonist-induced Ca^{2+} influx along with membrane cholesterol levels are reduced in PAECs from rats exposed to CH. This impaired agonist-induced Ca^{2+} influx in PAECs can be restored by both membrane cholesterol supplementation and by administration of a caveolin-1 scaffolding domain peptide (38). The number and structure of caveolae, however, are not altered in PAECs from CH rats compared with control rats (38). These data suggest that cholesterol per se may affect Ca^{2+} entry in these cells. However, questions remain as to whether cholesterol directly modulates endothelial agonist-induced Ca^{2+} entry and whether its major components, SOCE and depolarization-induced Ca^{2+} entry, are differentially affected.

The membrane cholesterol-depleting agent methyl-β-cyclodextrin (MβCD) has been used to investigate the importance of membrane cholesterol in cellular signaling pathways (59). However, by removing membrane cholesterol, MβCD can also

Address for reprint requests and other correspondence: T. C. Resta, Dept. of Cell Biology and Physiology, Univ. of New Mexico Health Sciences Center, MSC 08-4750, 1 Univ. of New Mexico, Albuquerque, NM 87131-0001 (e-mail: TResta@salud.unm.edu).

disrupt caveolar structure (40). Consequently, this approach often raises the question of whether membrane cholesterol regulates signaling pathways by direct interaction with membrane proteins or rather by altering the properties of lipid microdomains. To address this problem, the enantiomer of cholesterol (epicholesterol), which has similar effects on membrane fluidity and lipid domain formation as those of cholesterol but lacks the regulatory influences of cholesterol on ion channel function, has been used as a tool to study cholesterol-ion channel interactions (1a, 19, 28, 57). In the present study, we hypothesized that *1*) membrane cholesterol facilitates SOCE and depolarization-induced Ca^{2+} entry in PAECs and *2*) reduced endothelial Ca^{2+} influx after CH is due to loss of membrane cholesterol. We tested this hypothesis by examining the effect of either membrane cholesterol supplementation or cholesterol substitution with epicholesterol on endothelial Ca^{2+} entry in freshly isolated PAECs from normoxic and CH rats.

METHODS

Animals and CH exposure protocol. Male Sprague-Dawley rats (200–250 g) were used for all experiments. Rats exposed to CH were placed in a hypobaric chamber with barometric pressure maintained at ≈380 Torr for 4 wk. Age-matched control rats were housed in similar cages under ambient barometric pressure (≈630 Torr). The hypobaric chamber was opened 3 times/wk to provide fresh rat chow, water, and clean bedding. All animals were maintained on a 12:12-h light-dark cycle. All protocols used in this study were reviewed and approved by the Institutional Animal Care and Use Committee of the University of New Mexico Health Sciences Center.

Preparation of cholesterol and epicholesterol solutions. MβCD is a cyclic oligomer of glucose that, when saturated with either cholesterol or epicholesterol, can effectively deliver these sterols to the plasma membrane (19). This approach has been used to enrich or substitute endogenous membrane cholesterol in neurons (51) and aortic endothelial cells (46). MβCD-cholesterol or -epicholesterol complexes were generated as previously described (9). Briefly, cyclodextrin-sterol solutions were prepared by the addition of sterols to MβCD (10 mM) at a molar ratio of 1:5 and dissolution in HEPES buffer containing the following (in mM): 150.0 NaCl, 6.0 KCl, 1.0 $MgCl_2$, 1.8 $CaCl_2$, 10.0 HEPES, and 10.0 glucose (pH 7.4). Each solution was vortexed and sonicated using a bath sonicator for 10–15 min. The saturated cyclodextrin-sterol solution was then placed in a rotating incubator at 37°C overnight. This stock solution was filtered through a 0.22-μm syringe filter, aliquoted, and stored at −80°C.

Isolation and preparation of PAECs. After CH or normoxic exposure, rats were euthanized with pentobarbital sodium (200 mg/kg ip), and the heart and lungs were exposed by midline thoracotomy. The left lung was rapidly excised and placed in ice-cold HEPES buffer solution. Intrapulmonary arteries (third and fourth order, 200- to 400-μm inner diameter) were dissected from the superior region of the left lung, and the parenchymal lung tissue was carefully removed. Arteries were then cut longitudinally and treated with 0.2 mg/ml dithiothreitol and 2 U/ml papain in HEPES buffer for 45 min at 37°C. Vessels were carefully removed from the digestion solution and placed in 1 ml HEPES buffer containing 2 mg/ml BSA. PAEC sheets were then released by gentle trituration with a small-bore fire-polished Pasteur pipette and stored at 4°C. One to two drops of the solution containing freshly isolated rat PAECs were placed on a poly-L-lysine-coated glass coverslip and incubated at 37°C in the presence of vehicle, cholesterol, or epicholesterol. Cholesterol supplementation was performed in previously untreated endothelial sheets isolated from rats by incubation with cholesterol-MβCD (Chol:MβCD) solution for 30 min at 37°C. Epicholesterol substitution was similarly achieved by incubating isolated PAECs with epicholesterol-MβCD (EpiChol:MβCD) solution for 30 min at 37°C. All experiments were performed under normoxic conditions.

Membrane cholesterol content. Rat PAECs were freshly isolated and prepared on poly-L-lysine-coated glass coverslips before treatment with vehicle, cholesterol, or epicholesterol. Briefly, cholesterol supplementation and epicholesterol substitution were performed by incubating PAECs with Chol:MβCD or EpiChol:MβCD solutions, respectively, for 30 min at 37°C. Treated PAECs were then washed with PBS and fixed with 2% paraformaldehyde in PBS for 15 min at room temperature. Endothelial cell membrane cholesterol was detected by incubating cells with the fluorescent cholesterol marker filipin III (20 μg/ml, Sigma) for 15 min at room temperature under light-protected conditions, and coverslips were mounted on the slides using mounting media (38). Slides were air dried at 4°C and stored at −20°C until analysis. Samples were imaged by fluorescence confocal microscopy (Zeiss LSM 510 AxioObserver) using a 405-nm laser (excitation), 420-nm long-pass filter (emission) and Plan-Neofluor ×40/1.3 oil objective. Filipin staining was quantified using ImageJ (National Institutes of Health). A total of 25–100 cells/rat were analyzed. Fluorescence intensity was quantified by setting a threshold using blank control (filipin-untreated group). The fluorescence of each PAEC sheet was calculated and averaged to determine mean fluorescence for each animal.

Endothelial caveolar number. Cultured rat pulmonary microvascular endothelial cells (PMVECs, *passage 6*, cultured in MCDB-131 complete media, VEC Technologies) were treated with vehicle, MβCD, Chol:MβCD, or EpiChol:MβCD at 37°C for 30 min. Cells were washed in HEPES buffer for 10 min and prepared for transmission electron microscopy by fixation with 3.0% formaldehyde, 2.0% glutaraldehyde, and 1.5 mM $CaCl_2$ in 0.1 M sodium cacodylate buffer. Cells were postfixed in reduced osmium tetroxide (1.0% OsO_4 and 0.5% potassium ferrocyanide), dehydrated, embedded in epoxy resin, sectioned, and stained with uranyl acetate (saturated, aqueous).

Caveolae between 60 and 100 nm in diameter were counted at the membrane of endothelial cells and divided by the length of cell membrane in microns using ImageJ software. A total of 100 images encompassing 38 cells and 438 μm of membrane were analyzed by a person who was blinded to treatment.

Endothelial fura-2 loading. After vehicle, cholesterol, or epicholesterol treatment, freshly isolated PAEC sheets were plated and loaded with fura-2 AM (3.00 μM and 0.05% pluronic acid) in HEPES buffer for 7 min at room temperature (~23°C) and washed for 15 min at 37°C. Ratiometric changes in endothelial cell $[Ca^{2+}]_i$ were determined by alternating a xenon arc lamp light source between 340- and 380-nm band-pass filters at 1 Hz (Ionoptix Hyperswitch), and the interleaved fura-2 fluorescence emissions at 510 nm were detected with a photomultiplier tube.

Agonist-induced Ca^{2+} influx and SOCE in freshly isolated endothelial cells. Agonist-induced Ca^{2+} influx and SOCE were measured in PAEC sheets as previously described (38). After being loaded with fura-2 loading and washed, fura-2-loaded endothelial sheets were superfused with Ca^{2+}-free HEPES buffer for 5 min and then stimulated with ATP (20 μM) or cyclopiazonic acid [CPA; sarco(endo) plasmic reticulum Ca^{2+}-ATPase inhibitor, 10 μM] to deplete intracellular Ca^{2+} stores. Ca^{2+} entry was then induced by repletion of extracellular Ca^{2+} (1.8 mM) in the continued presence of ATP or CPA. Ca^{2+} influx was quantified as the area under the curve (AUC) for the 5 min after the reintroduction of extracellular Ca^{2+}.

Measurement of PAEC membrane potential. Endothelial membrane potential (E_m) was measured in en face small pulmonary arteries superfused with physiological salt solution (37°C, equilibrated with 10% O_2 and 6% CO_2) using glass microelectrodes (tip resistance: 40–80 MΩ) filled with 3 M KCl. A Neuroprobe amplifier (A-M Systems) was used to record E_m. Analog output from the amplifier was low-pass filtered at 1 kHz and recorded and analyzed

using Axoscope software (Axon Instruments). E_m was measured under baseline conditions and in response to 10 μM ATP. Criteria for acceptance of E_m recordings included *1*) an abrupt negative deflection of potential as the microelectrode was advanced into a cell, *2*) a stable E_m for at least 1 min, and *3*) an abrupt change in potential to 0 mV after the electrode was retracted from the cell.

Depolarization-induced Ca^{2+} influx in freshly isolated endothelial cells. The ratiometric changes in fura-2 fluorescence represent the sum of changes in $[Ca^{2+}]_i$, which includes Ca^{2+} influx, Ca^{2+} uptake by organelles, and Ca^{2+} extrusion from the cell. To specifically assess Ca^{2+} entry, Mn^{2+} is used as a Ca^{2+} surrogate because of its unique property to traverse most Ca^{2+}-permeable channels (2), irreversibly bind to fura-2, and quench fura-2 fluorescence (wavelength at ~360 nm). Endothelial cell depolarization-induced Ca^{2+} influx was determined by Mn^{2+} quenching of fura-2 fluorescence in freshly isolated PAEC sheets as previously described (39). This preparation was excited at the isosbestic wavelength (360 nm), and emission was recorded at 510 nm. Similar to the previous protocol, fura-2-loaded endothelial sheets were superfused with Ca^{2+}-free HEPES buffer for 5 min and administered KCl (60 mM) to elicit membrane depolarization. Ca^{2+} entry represented by the influx of the Ca^{2+} surrogate Mn^{2+} was then determined upon addition of extracellular Mn^{2+} (500 μM) in the continued presence of KCl. Depolarization-induced Ca^{2+} entry was quantified by the percentage of the Mn^{2+}-quenched fluorescence at 90 s after administration of Mn^{2+}.

Calculations and statistics. All data are expressed as means ± SE. Values of *n* refer to the numbers of cells for experiments examining caveolar number or to the number of animals for other experiments. Percentage data were converted to normal distributions by arcsine transformation before parametric analysis. An unpaired *t*-test, one-way ANOVA, two-way ANOVA, or Kruskal-Wallis *H*-test were used where appropriate for statistical comparisons. If differences were detected by ANOVA or the Kruskal-Wallis *H*-test, individual groups were compared with the Student-Newman-Keuls or Dunn's multiple-comparison tests, respectively. *P* values of <0.05 were accepted as statistically significant for all comparisons.

RESULTS

Effect of cholesterol manipulation on endothelial membrane cholesterol content. Filipin is a polyene antibiotic that binds to membrane cholesterol via hydrophobic interactions (36) but cannot bind to epicholesterol (13). Consistent with our previously published data (38), filipin fluorescence was less in cells from CH rats compared with normoxic rats (Fig. 1). Cholesterol supplementation restored diminished membrane cholesterol in cells from CH animals while having no effect in normoxic control animals. Furthermore, epicholesterol treatment significantly reduced filipin fluorescence in freshly isolated PAECs from both control and CH rats. These data suggest that epicholesterol treatment is an effective approach to substitute endogenous membrane cholesterol for epicholesterol in this preparation.

Effect of cholesterol manipulation on endothelial caveolar number. Effects of cholesterol depletion, supplementation, or substitution treatments on caveolar number and structure were examined in cultured rat PMVECs using transmission electron microscopy. MβCD, as a cholesterol carrier, can sequester membrane cholesterol and disrupt caveolar structure when used alone (20). Consistent with previous findings, MβCD decreased the incidence of caveolae (Fig. 2). In contrast, neither cholesterol supplementation nor epicholesterol substitution altered caveolar number compared with vehicle control. These results support an effect of epicholesterol treatment to substitute rather than deplete endogenous membrane cholesterol.

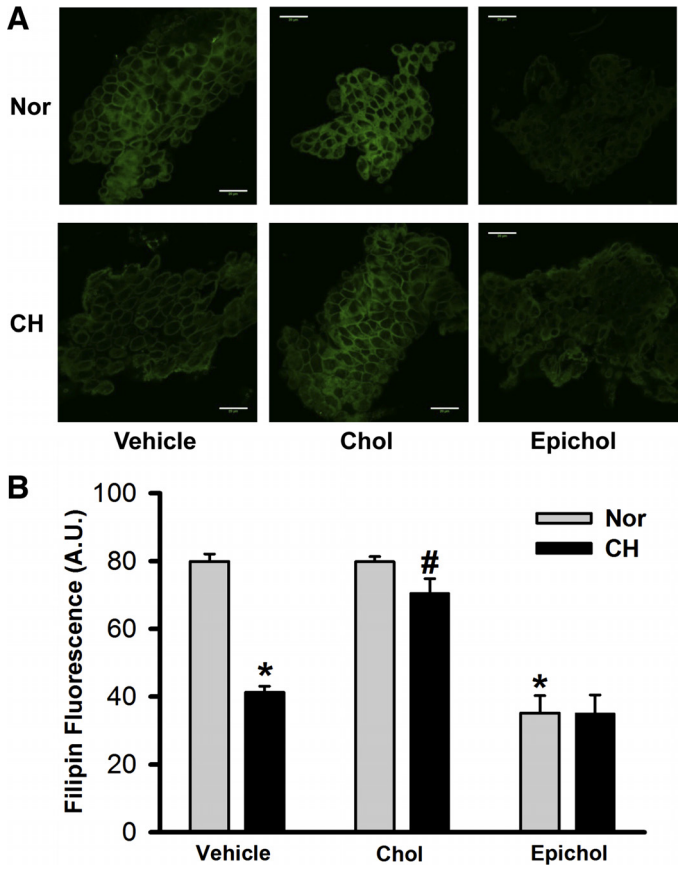

Fig. 1. Epicholesterol (Epichol) reduces endogenous membrane cholesterol (Chol) of freshly isolated pulmonary arterial endothelial cell (PAEC) sheets from both normoxic (Nor) and chronic hypoxic (CH) rats. *A*: representative images of membrane cholesterol indicated by filipin fluorescence in PAECs isolated from each group. Cells were pretreated with vehicle, Chol, or Epichol. Scale bars = 20 μm. *B*: mean filipin fluorescence [in arbitrary units (A.U.)] in PAEC sheets from each group. Two-way ANOVA followed by the Student-Newman-Keuls post hoc test was used to compare between groups. Values are means ± SE; $n = 3$ animals/group. $*P < 0.05$ vs. Nor vehicle; $\#P < 0.05$ vs. CH vehicle.

Epicholesterol substitution attenuates endothelial ATP-induced Ca^{2+} entry. ATP-induced Ca^{2+} entry and SOCE were assessed using ratiometric fura-2 measurement as previously described (37, 38). Ca^{2+} entry was quantified as the AUC for the 5 min after reintroduction of extracellular Ca^{2+} in the continued presence of ATP or CPA (Fig. 3). ATP-induced Ca^{2+} entry was diminished in isolated PAECs from normoxic rats after EpiChol:MβCD treatment compared with vehicle control rats but was not significantly altered by cholesterol supplementation (Chol:MβCD) (Fig. 4). These data suggest that endothelial membrane cholesterol is necessary for agonist-induced Ca^{2+} entry.

Cholesterol supplementation restores endothelial SOCE after CH. To assess the importance of membrane cholesterol in SOCE, we examined effects of cholesterol supplementation and epicholesterol substitution on CPA-induced Ca^{2+} influx in isolated PAECs. SOCE was diminished in cells from CH rats compared with control rats and was rescued by cholesterol repletion (Fig. 5). Furthermore, epicholesterol substitution

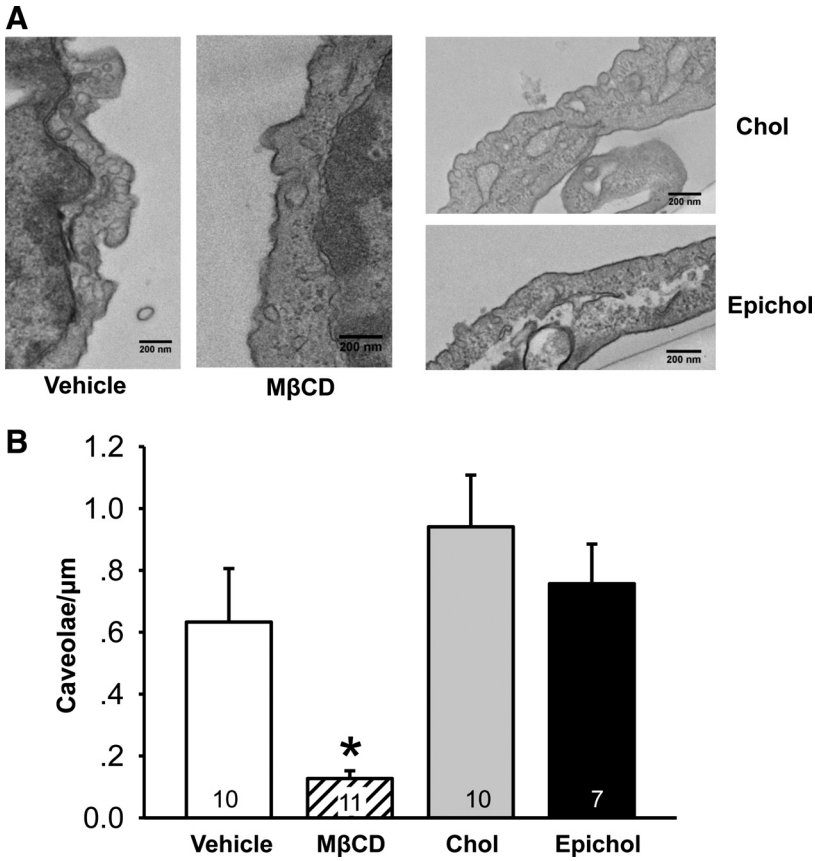

Fig. 2. Caveolae number is reduced by cholesterol depletion with methyl-β-cyclodextrin (MβCD) but not by Chol or Epichol treatment in cultured pulmonary microvascular endothelial cells (PMVECs). *A*: representative images of caveolae in cultured PMVECs from each treatment group. *B*: mean number of caveolae per length of cell membrane (caveolae/μm). Data were compared by the Kruskal-Wallis *H*-test and Dunn's multiple-comparison test. Values are means ± SE; n = 7–11 cells (indicated in bars). *$P < 0.05$ vs. all other treatments. A total of 100 images encompassing 38 cells and 438 μm of membrane were analyzed.

greatly inhibited CPA-induced Ca^{2+} entry in PAECs from both normoxic and CH rats compared with their respective vehicle controls.

ATP causes endothelial membrane depolarization. We have previously demonstrated that CH inhibits depolarization-induced Ca^{2+} entry in PAECs (39). However, it is unclear whether ATP elicits depolarization in these cells that could evoke this pathway. Consistent with this possibility, we found that ATP caused membrane depolarization in endothelium of freshly isolated pulmonary arteries from control rats (Fig. 6).

Decreased membrane cholesterol leads to reduced endothelial depolarization-induced Ca^{2+} entry after CH. Endothelial cell depolarization-induced Ca^{2+} influx was determined by Mn^{2+} quenching of fura-2 fluorescence in freshly isolated PAECs. Introduction of Mn^{2+} caused a steady decline in fura-2 fluorescence in the absence of KCl in PAECs from both control and CH rats, indicative of basal Ca^{2+} entry (Fig. 7). A depolarizing stimulus of KCl (60 mM) increased entry of the Ca^{2+} surrogate in isolated PAECs from control rats. However, this response to KCl was absent in PAECs from CH rats.

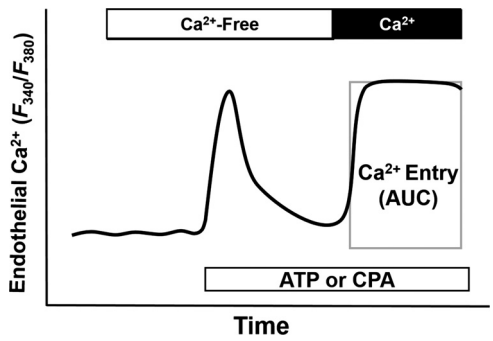

Fig. 3. Experimental protocol for measuring ATP- and cyclopiazonic acid (CPA)-induced Ca^{2+} entry in isolated PAEC sheets. Depletion of the intracellular Ca^{2+} store was induced by 20 μM ATP or 10 μM CPA in Ca^{2+}-free HEPES buffer. Intracellular Ca^{2+} was expressed as the fura-2 340-to-380-nm emission ratio. Ca^{2+} entry was assessed by calculating the area under the curve (AUC) for the 5 min after the reintroduction of extracellular Ca^{2+} (indicated by the rectangle).

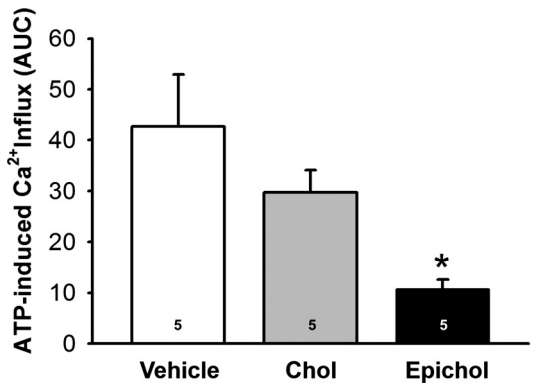

Fig. 4. Epichol substitution reduces ATP-induced Ca^{2+} entry in PAEC sheets from Nor rats. Ca^{2+} influx was assessed by ratiometric analysis of fura-2 fluorescence. One-way ANOVA followed by the Student-Newman-Keuls test was used to compare between groups. Values are means ± SE; n = 5 animals/group. *$P < 0.05$ vs. vehicle.

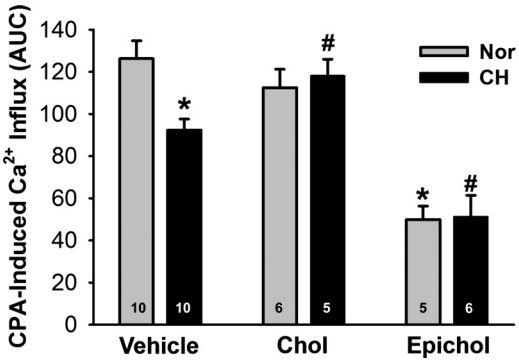

Fig. 5. Decreased membrane Chol leads to reduced endothelial store-operated Ca^{2+} entry after CH. Ca^{2+} influx was assessed by ratiometric analysis of fura-2 fluorescence in PAEC sheets. Chol supplementation restored CPA-induced Ca^{2+} entry after CH, whereas Epichol substitution significantly inhibited CPA-induced Ca^{2+} entry in PAEC sheets from both Nor and CH rats. Groups were compared by two-way ANOVA followed by multiple-comparison testing using the Student-Newman-Keuls test. Values are means ± SE; n = 5–10 animals/group (indicated in bars). *$P < 0.05$ vs. Nor vehicle; #$P <$ 0.05 vs. CH vehicle.

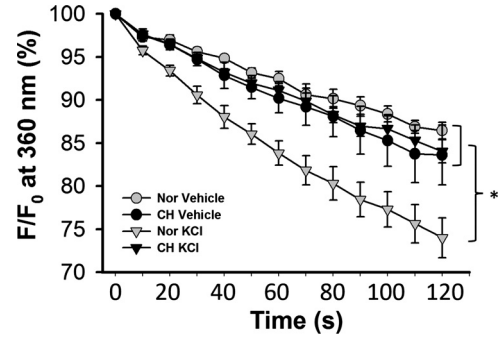

Fig. 7. Exposure to CH abolishes endothelial depolarization-induced Ca^{2+} entry. A measure of endothelial Ca^{2+} entry was assessed by Mn^{2+} quenching of fura-2 fluorescence in PAEC sheets from control and CH rats treated with either vehicle (time control) or 60 mM KCl (depolarizing stimulus). F, fluorescence intensity at 360 nm excitation; F_0, fluorescence intensity at *time 0*. Two-way ANOVA and the Student-Newman-Keuls test were used to compare between groups at each time point. Values are means ± SE; n = 5 with Nor vehicle, n = 5 with CH vehicle, n = 7 with Nor KCl, and n = 6 with CH KCl. *$P < 0.05$ vs. Nor KCl over the range of 20–120 s.

To confirm the involvement of T-type VGCCs in depolarization-induced Ca^{2+} influx (39), we repeated these experiments in the presence of the L-type Ca^{2+} channel inhibitor diltiazem or the T-type inhibitor mibefradil. Whereas diltiazem did not affect responses to KCl in cells from either normoxic or CH rats, mibefradil abolished KCl-induced Mn^{2+} quenching of fura-2 fluorescence in PAECs from normoxic control rats while having no effect in cells from CH rats (Fig. 8).

Consistent with a requirement for membrane cholesterol in depolarization-induced Ca^{2+} entry, epicholesterol substitution prevented depolarization-induced Mn^{2+} entry in PAECs from normoxic rats, whereas cholesterol supplementation was without effect in these cells (Fig. 9). In addition, cholesterol repletion partially restored the KCl-induced Mn^{2+} influx in PAECs from CH rats, suggesting that reduced membrane cholesterol contributes to impaired depolarization-induced Ca^{2+} entry after CH.

DISCUSSION

Our laboratory has previously shown that reduced membrane cholesterol after CH is associated with decreased ATP-induced Ca^{2+} entry in intrapulmonary artery endothelial cells. However, it is unclear whether membrane cholesterol regulates endothelial Ca^{2+} entry through direct interactions with signaling molecules or through changes in physical properties of the plasma membrane. The goal of the present study was to determine the contribution of membrane cholesterol to agonist-induced Ca^{2+} entry and its major components, SOCE and Ca^{2+} entry through VGCCs. The major findings from this study are that substitution of endogenous membrane cholesterol with its epimer, epicholesterol, attenuates ATP-induced Ca^{2+} entry, SOCE, and depolarization-induced Ca^{2+} entry in PAECs. In addition, decreased endothelial SOCE and depolarization-induced Ca^{2+} entry after CH are largely restored by cholesterol supplementation. However, neither cholesterol supplementation nor epicholesterol substitution alters endothelial caveolar number and structure. The results from this study suggest that membrane cholesterol directly regulates agonist-induced Ca^{2+} entry and its components and further demonstrate that impaired endothelial Ca^{2+} entry after CH is due to altered membrane cholesterol homeostasis. These findings pro-

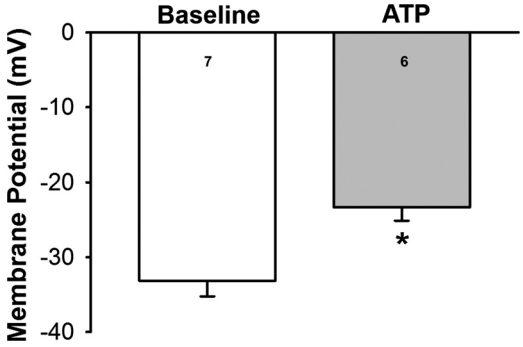

Fig. 6. ATP induces membrane depolarization in the pulmonary artery endothelium. Endothelial membrane potential was measured under baseline conditions and in response to 10 μM ATP in en face small pulmonary arteries from control rats. An unpaired t-test was used to compare between two groups. Values are means ± SE; n = 7 for baseline and n = 6 with ATP (3–6 membrane potential recordings were conducted per artery and averaged for an n = 1). *$P < 0.05$ vs. baseline.

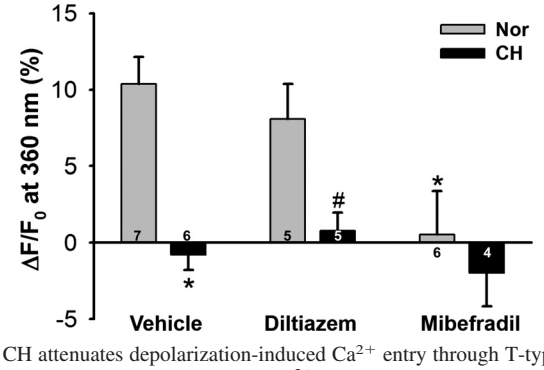

Fig. 8. CH attenuates depolarization-induced Ca^{2+} entry through T-type Ca^{2+} channels in PAECs. Data represent Mn^{2+}-quenched fura-2 fluorescence (at 90-s time point) in response to KCl (60 mM) in PAEC sheets from control and CH rats. Diltiazem (50 μM) and mibefradil (10 μM) were used to selectively inhibit L-type and T-type Ca^{2+} channels, respectively. Data are expressed as $\Delta F/F_0$ (in %) from the time control. Two-way ANOVA and the Student-Newman-Keuls test were used to compare between groups. Values are means ± SE; n = 4–7 animals/group (indicated in bars). *$P < 0.05$ vs. Nor vehicle; #$P < 0.05$ vs. Nor diltiazem.

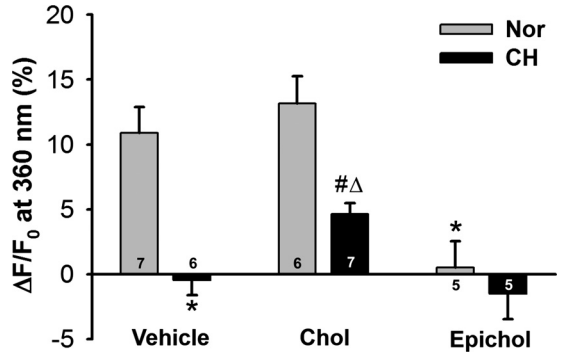

Fig. 9. Decreased membrane cholesterol leads to reduced endothelial depolarization-induced Ca^{2+} entry after CH. Data represent Mn^{2+}-quenched fura-2 fluorescence (at 90-s time point) in response to KCl (60 mM) in PAEC sheets from control and CH rats. Chol repletion partially restored depolarization-induced Ca^{2+} entry after CH. Epichol greatly inhibited KCl-induced Ca^{2+} entry in PAECs from both Nor and CH rats. Data are expressed as $\Delta F/F_0$ (in %) from the time control. Statistical comparisons were made using two-way ANOVA and the Student-Newman-Keuls post hoc test. Values are means ± SE; n = 5–7 animals/group (indicated in bars). *$P < 0.05$ vs. Nor vehicle; #$P < 0.05$ vs. Nor chol; $\Delta P < 0.05$ vs. CH vehicle.

vide an enhanced mechanistic understanding of factors that contribute to endothelial dysfunction and the associated pulmonary hypertension (PH) resulting from long-term hypoxic exposure.

Many cells release ATP in response to mechanical signals, including shear stress, extracellular fluid movement, and changes in cell volume (15, 52, 58). The activation of G protein-coupled purinergic receptors by endogenous ATP may regulate myogenic tone and vascular remodeling (14, 24). In endothelial cells, shear stress-induced production of ATP serves as an autocrine factor and stimulates endothelial NO production (3). ATP as an agonist achieves its various roles through controlling intracellular Ca^{2+}. The binding of an agonist to its receptor mediates the activation of phospholipase C and production of inositol 1,4,5-trisphosphate (IP_3). Cytosolic IP_3 then binds to IP_3 receptors on the endoplasmic reticulum (ER), leading to depletion of the ER Ca^{2+} store and subsequent SOCE (45). Agonist binding may also elicit Ca^{2+} entry through receptor-operated cation channels that are activated independently of store emptying (48). Purinergic agonists may further mediate depolarization-induced Ca^{2+} entry through VGCCs secondary to activation of various nonselective cation channels, including transient receptor potential canonical (TRPC) channels and the ionotropic P2X receptor (10). Interestingly, membrane cholesterol appears to be a key determinant of agonist-induced Ca^{2+} influx in vascular smooth muscle (43, 44) and the endothelium (38), possibly through regulation of Ca^{2+}-permeable ion channels.

Direct interaction between sterols and ion channels has been suggested by the sensitivity of inwardly rectifying K^+ (K_{ir}) channels (46) and large-conductance Ca^{2+}-activated K^+ (BK_{Ca}) channels (7) to various sterol analogs. In addition, cholesterol-binding regions exist in both K_{ir} channels and BK_{Ca} channels (49, 50). However, the effect of membrane cholesterol on ion channel function may vary depending on the type of ion channel. For example, whereas cholesterol decreases the open probability of many K^+ channels, VGCCs, and voltage-gated Na^+ channels (12, 26, 53), other ion channels, such as epithelial Na^+ channels and TRPC channels, are inhibited by removal of membrane cholesterol (4, 5, 25). Regulation of ion channels involved in SOCE by changes in membrane cholesterol has been implicated in different cell types in previous studies (5, 18), in which membrane cholesterol depletion using MβCD impaired SOCE. However, the effect of membrane cholesterol in regulation of endothelial depolarization-induced Ca^{2+} entry has not been specifically investigated.

The importance of membrane cholesterol in agonist-induced Ca^{2+} entry has been suggested in cultured vascular smooth muscle cells, in which cholesterol enrichment augments agonist-induced Ca^{2+} influx (6). Our previous findings that cholesterol repletion enhances impaired ATP-induced Ca^{2+} entry in PAECs after CH (38) suggest that membrane cholesterol facilitates endothelial agonist-induced Ca^{2+} entry. ATP induces both SOCE and T-type VGCC blocker-sensitive Ca^{2+} influx in PAECs (39). In the present study, we confirmed that ATP causes membrane depolarization in the pulmonary artery endothelium, which leads to T-type channel activation and Ca^{2+} influx. Considering that SOCE and depolarization-induced Ca^{2+} entry are major components of ATP-induced Ca^{2+} entry and that both Ca^{2+} influx pathways are blunted after CH (37, 39), it is possible that membrane cholesterol also regulates these two components of the ATP-induced Ca^{2+} response.

Given the wide range of effects of mβCD, such as altering caveolar structure and disrupting other lipid microdomains (20), the direct contribution of membrane cholesterol to regulation of ion channels remains unclear. To investigate the direct role of membrane cholesterol in mediating endothelial Ca^{2+} influx, we used epicholesterol, the enantiomer of cholesterol, to substitute membrane cholesterol. Using epicholesterol to substitute endogenous cholesterol, we demonstrated a direct role of membrane cholesterol to facilitate ATP-induced Ca^{2+} entry in PAECs. Our data are consistent with findings that depletion of membrane cholesterol impairs this Ca^{2+} response in PAECs (38). We also provide evidence that SOCE, as the major component of the ATP-induced Ca^{2+} response, is similarly regulated by membrane cholesterol. This observation implies that membrane cholesterol may either directly affect store-operated cation channels (SOCs) or interact with a signaling pathway that activates SOCs. The finding that reduced endothelial SOCE in pulmonary arteries after CH was acutely restored by membrane cholesterol supplementation suggests that CH limits SOCE by reducing membrane cholesterol rather than by decreasing ion channel expression. Although this study has not identified the specific cation channel(s) involved in pulmonary endothelial SOCE, candidates include TRPC1, TRPC4, and Orai1, each of which has been implicated in endothelial SOCE and demonstrates cholesterol sensitivity (1, 5, 11, 31). Interestingly, both SOCE and receptor-operated Ca^{2+} entry in response to the P_2Y receptor agonist UTP are reduced in pulmonary artery smooth muscle cells after CH (23). This raises an interesting question of whether CH impairs agonist-induced Ca^{2+} influx in pulmonary artery smooth muscle cells through depletion of membrane cholesterol, similar to that presently observed in PAECs.

Wu et al. (55) first demonstrated that cultured rat PMVECs express mRNA of $Ca_v3.1$ and possess voltage-dependent currents that are sensitive to T-type channel blockers. They also reported that T-type VGCCs contribute to both agonist-induced Ca^{2+} entry and SOCE in PMVECs. Although T-type VGCCs

are not found in cultured rat PAECs (55), their expression and function are described in freshly dispersed rat PAECs (39). Paffett et al. (39) showed that T-type VGCCs contribute to depolarization-induced Ca^{2+} entry and receptor-operated Ca^{2+} entry in response to ATP. After exposure to CH, the mibefradil-sensitive component of ATP-induced Ca^{2+} entry is greatly reduced. The effect of CH on this Ca^{2+} entry is not due to altered membrane K^+ permeability because the impaired endothelial depolarization-induced Ca^{2+} entry after CH persists even when membrane K^+ permeability is equivalently clamped by the K^+ ionophore valinomycin. These findings suggest that T-type VGCCs are important mediators of depolarization-induced Ca^{2+} entry and that impaired Ca^{2+} entry via these channels may contribute to reduced basal $[Ca^{2+}]_i$ in PAECs after CH (39). Using the Mn^{2+}-quenching technique to selectively assess Ca^{2+} entry, we confirmed that depolarization-induced Ca^{2+} entry was sensitive to T-type VGCC inhibition and Ca^{2+} entry was eliminated after CH. Additionally, depolarization-induced Ca^{2+} entry after CH was partially restored by cholesterol supplementation. A similar effect of cholesterol on VGCCs has been reported in other cell types (56). Although studies on cholesterol regulation of VGCCs are limited, our finding that epicholesterol substitution abolished depolarization-induced Ca^{2+} entry in control cells suggests that there may be a direct interaction between membrane cholesterol and T-type VGCCs.

Although epicholesterol has effects similar to cholesterol on physical properties of the cell membrane (57), few studies have examined the effect of EpiChol:MβCD on caveolae. Here, we provide evidence that MβCD alone nearly abolished the incidence of caveolae, whereas neither Chol:MβCD nor EpiChol:MβCD affected caveolar number in cultured PMVECs. It has previously been shown that administration of an EpiChol:MβCD solution to bovine aortic endothelial cells effectively substitutes epicholesterol for endogenous membrane cholesterol (47). To verify this observation in our preparation, we assessed effects of epicholesterol substitution on membrane cholesterol content in freshly isolated PAECs using the fluorescent cholesterol marker filipin. Epicholesterol does not interact with filipin because of a different orientation of the 3-hydroxyl group compared with cholesterol (13, 36). As expected, we found that epicholesterol treatment greatly decreased filipin fluorescence intensity in isolated PAECs from both normoxic and CH rats, consistent with epicholesterol substitution of endogenous membrane cholesterol. In addition, cholesterol treatment restored membrane cholesterol content in PAECs from CH rats to the level of normoxic controls, consistent with our previous findings (38). These results suggest that EpiChol:MβCD treatment substitutes endogenous membrane cholesterol for epicholesterol without disrupting caveolae. Consequently, the observed effects of epicholesterol treatment on Ca^{2+} influx are likely due to loss of ion channel regulation by cholesterol, rather than to changes in caveolar density.

Two potential mechanisms of decreased membrane cholesterol after CH include *1*) inhibition of de novo cholesterol biosynthesis and *2*) membrane cholesterol oxidation. Mukodani et al. (30) first reported that hypoxia induces lipid accumulation and impairs cholesterol synthesis in cultured rabbit skin fibroblasts. The mechanism by which hypoxia affects cholesterol synthesis was later explored by Nguyen et al. (35). They reported that hypoxia induces accumulation of cholesterol biosynthetic intermediates and activates HIF-1α-mediated induction of the ER membrane proteins Insig-1 and Insig-2. These responses lead to rapid degradation of 3-hydroxy-3-methylglutaryl-CoA reductase and subsequently limit cholesterol synthesis (35). Chronic hypoxia can also increase the production of reactive oxygen species (ROS) (17, 27), which may facilitate membrane cholesterol oxidation. Because filipin cannot be used to label oxidized cholesterol (42), it is possible that reduced filipin staining in PAECs from CH rats reflects membrane cholesterol oxidation by ROS. Cholesterol oxidation, not only has potential to disrupt the interaction between cholesterol and ion channels and other regulatory proteins but also may inhibit de novo cholesterol synthesis (33). Future studies are required to evaluate the potential contributions of these mechanisms to reduced PAEC membrane cholesterol after CH.

Our finding that CH attenuates agonist-dependent Ca^{2+} influx pathways in PAECs does not preclude a potential effect of CH to modify other intracellular Ca^{2+}-regulatory mechanisms, including ER sequestration or plasmalemmal efflux pathways. However, decreased endothelial ATP-induced Ca^{2+} influx after CH is not associated with changes in ATP-induced Ca^{2+} mobilization (38), suggesting that this attenuated Ca^{2+} entry is not due to altered Ca^{2+} release or Ca^{2+} loading of the ER. It should also be noted that impaired Ca^{2+} entry after CH observed in endothelial cells from larger parenchymal pulmonary arteries may not be reflective of smaller arteries that likely provide a greater contribution to regulation of vascular resistance in hypertensive pulmonary circulation. Future studies are needed to evaluate whether these effects of CH to alter calcium influx pathways are conserved across the pulmonary circulation and the impact of these responses on the development of CH-induced PH.

In conclusion, the present study provides evidence that membrane cholesterol facilitates pulmonary endothelial Ca^{2+} entry likely through interaction with membrane ion channels. Our findings also demonstrate that impaired SOCE and depolarization-induced Ca^{2+} entry after CH are associated with reduced membrane cholesterol levels and are restored by cholesterol supplementation. This membrane cholesterol-associated decrease in endothelial Ca^{2+} entry after CH may not only affect regulation of vascular tone but also has potentially broader implications for cholesterol regulation of endothelial migration, proliferation, and apoptosis. Our study contributes to the understanding of the effect of CH on membrane cholesterol homeostasis and the subsequent impact on endothelial $[Ca^{2+}]_i$ in pulmonary arteries, which could shed light on developing potential therapeutic treatments for pulmonary hypertension that target membrane cholesterol. Future studies will focus on identifying specific ion channels that interact with membrane cholesterol in pulmonary endothelial cells.

ACKNOWLEDGMENTS

We thank Tamara Howard for the generation of electron micrographs and Minerva Murphy for technical assistance.

GRANTS

This work was supported by National Heart, Lung, and Blood Institute Grants R01-HL-95640 (to B. R. Walker) and R01-HL-132883 and R01-HL-088192 (to T. C. Resta) and by American Heart Association Grants 15GRNT21080001 (to B. R. Walker) and 16GRNT27700010 (to T. C. Resta).

DISCLOSURES

No conflicts of interest, financial or otherwise, are declared by the authors.

AUTHOR CONTRIBUTIONS

B.Z., J.S.N., N.L.J., B.R.W., and T.C.R. conceived and designed research; B.Z. and J.S.N. performed experiments; B.Z. and J.S.N. analyzed data; B.Z., J.S.N., N.L.J., B.R.W., and T.C.R. interpreted results of experiments; B.Z. and J.S.N. prepared figures; B.Z. drafted manuscript; B.Z., J.S.N., N.L.J., B.R.W., and T.C.R. edited and revised manuscript; B.Z., J.S.N., N.L.J., B.R.W., and T.C.R. approved final version of manuscript.

REFERENCES

1. **Abdullaev IF, Bisaillon JM, Potier M, Gonzalez JC, Motiani RK, Trebak M.** Stim1 and Orai1 mediate CRAC currents and store-operated calcium entry important for endothelial cell proliferation. *Circ Res* 103: 1289–1299, 2009. doi:10.1161/01.RES.0000338496.95579.56.

1a. **Alakoskela JM, Sabatini K, Jiang X, Laitala V, Covey DF, Kinnunen PKJ.** Enantiospecific interactions between cholesterol and phospholipids. *Langmuir* 24: 830–836, 2008. doi:10.1021/la702909q.

2. **Anderson M.** Mn ions pass through calcium channels. A possible explanation. *J Gen Physiol* 81: 805–827, 1983. doi:10.1085/jgp.81.6.805.

3. **Andrews AM, Jaron D, Buerk DG, Barbee KA.** Shear stress-induced NO production is dependent on ATP autocrine signaling and capacitative calcium entry. *Cell Mol Bioeng* 7: 510–520, 2014. doi:10.1007/s12195-014-0351-x.

4. **Barberà JA, Peinado VI, Santos S.** Pulmonary hypertension in chronic obstructive pulmonary disease. *Eur Respir J* 21: 892–905, 2003. doi:10.1183/09031936.03.00115402.

5. **Bergdahl A, Gomez MF, Dreja K, Xu SZ, Adner M, Beech DJ, Broman J, Hellstrand P, Swärd K.** Cholesterol depletion impairs vascular reactivity to endothelin-1 by reducing store-operated Ca^{2+} entry dependent on TRPC1. *Circ Res* 93: 839–847, 2003. doi:10.1161/01.RES.0000100367.45446.A3.

6. **Bialecki RA, Tulenko TN, Colucci WS.** Cholesterol enrichment increases basal and agonist-stimulated calcium influx in rat vascular smooth muscle cells. *J Clin Invest* 88: 1894–1900, 1991. doi:10.1172/JCI115512.

7. **Bukiya AN, Belani JD, Rychnovsky S, Dopico AM.** Specificity of cholesterol and analogs to modulate BK channels points to direct sterol-channel protein interactions. *J Gen Physiol* 137: 93–110, 2011. doi:10.1085/jgp.201010519.

8. **Busse R, Mülsch A.** Calcium-dependent nitric oxide synthesis in endothelial cytosol is mediated by calmodulin. *FEBS Lett* 265: 133–136, 1990. doi:10.1016/0014-5793(90)80902-U.

9. **Christian AE, Haynes MP, Phillips MC, Rothblat GH.** Use of cyclodextrins for manipulating cellular cholesterol content. *J Lipid Res* 38: 2264–2272, 1997.

10. **Chung HS, Park KS, Cha SK, Kong ID, Lee JW.** ATP-induced $[Ca^{2+}]_i$ changes and depolarization in GH3 cells. *Br J Pharmacol* 130: 1843–1852, 2000. doi:10.1038/sj.bjp.0703253.

11. **Cioffi DL, Wu S, Stevens T.** On the endothelial cell I_{SOC}. *Cell Calcium* 33: 323–336, 2003. doi:10.1016/S0143-4160(03)00046-0.

12. **Crowley JJ, Treistman SN, Dopico AM.** Cholesterol antagonizes ethanol potentiation of human brain BKCa channels reconstituted into phospholipid bilayers. *Mol Pharmacol* 64: 365–372, 2003. doi:10.1124/mol.64.2.365.

13. **Elias PM, Friend DS, Goerke J.** Membrane sterol heterogeneity. Freeze-fracture detection with saponins and filipin. *J Histochem Cytochem* 27: 1247–1260, 1979. doi:10.1177/27.9.479568.

14. **Erlinge D, Burnstock G.** P2 receptors in cardiovascular regulation and disease. *Purinergic Signal* 4: 1–20, 2008. doi:10.1007/s11302-007-9078-7.

15. **Fitz JG.** Regulation of cellular ATP release. *Trans Am Clin Climatol Assoc* 118: 199–208, 2007.

16. **Förstermann U, Pollock JS, Schmidt HH, Heller M, Murad F.** Calmodulin-dependent endothelium-derived relaxing factor/nitric oxide synthase activity is present in the particulate and cytosolic fractions of bovine aortic endothelial cells. *Proc Natl Acad Sci USA* 88: 1788–1792, 1991. doi:10.1073/pnas.88.5.1788.

17. **Fresquet F, Pourageaud F, Leblais V, Brandes RP, Savineau JP, Marthan R, Muller B.** Role of reactive oxygen species and $gp91^{phox}$ in endothelial dysfunction of pulmonary arteries induced by chronic hypoxia. *Br J Pharmacol* 148: 714–723, 2006. doi:10.1038/sj.bjp.0706779.

18. **Galan C, Woodard GE, Dionisio N, Salido GM, Rosado JA.** Lipid rafts modulate the activation but not the maintenance of store-operated Ca^{2+} entry. *Biochim Biophys Acta* 1803: 1083–1093, 2010. doi:10.1016/j.bbamcr.2010.06.006.

19. **Gimpl G, Burger K, Fahrenholz F.** Cholesterol as modulator of receptor function. *Biochemistry* 36: 10959–10974, 1997. doi:10.1021/bi963138w.

20. **Graziani A, Bricko V, Carmignani M, Graier WF, Groschner K.** Cholesterol- and caveolin-rich membrane domains are essential for phospholipase A_2-dependent EDHF formation. *Cardiovasc Res* 64: 234–242, 2004. doi:10.1016/j.cardiores.2004.06.026.

21. **Hinton JM, Langton PD.** Inhibition of EDHF by two new combinations of K^+-channel inhibitors in rat isolated mesenteric arteries. *Br J Pharmacol* 138: 1031–1035, 2003. doi:10.1038/sj.bjp.0705171.

23. **Jernigan NL, Broughton BR, Walker BR, Resta TC.** Impaired NO-dependent inhibition of store- and receptor-operated calcium entry in pulmonary vascular smooth muscle after chronic hypoxia. *Am J Physiol Lung Cell Mol Physiol* 290: L517–L525, 2006. doi:10.1152/ajplung.00308.2004.

24. **Koltsova SV, Maximov GV, Kotelevtsev SV, Lavoie JL, Tremblay J, Grygorczyk R, Hamet P, Orlov SN.** Myogenic tone in mouse mesenteric arteries: evidence for P2Y receptor-mediated, Na^+,K^+,$2Cl^-$ cotransport-dependent signaling. *Purinergic Signal* 5: 343–349, 2009. doi:10.1007/s11302-009-9160-4.

25. **Kwiatek AM, Minshall RD, Cool DR, Skidgel RA, Malik AB.** Caveolin-1 regulates store-operated Ca^{2+} influx by binding of its scaffolding domain to transient receptor potential channel-1 in endothelial cells. *Mol Pharmacol* 70: 1174–1183, 2006. doi:10.1124/mol.105.021741.

26. **Lin M-W, Wu AZ, Ting W-H, Li C-L, Cheng K-S, Wu S-N.** Changes in membrane cholesterol of pituitary tumor (GH3) cells regulate the activity of large-conductance Ca^{2+}-activated K^+ channels. *Chin J Physiol* 49: 1–13, 2006.

27. **Liu JQ, Zelko IN, Erbynn EM, Sham JSK, Folz RJ.** Hypoxic pulmonary hypertension: role of superoxide and NADPH oxidase ($gp91^{phox}$). *Am J Physiol Lung Cell Mol Physiol* 290: L2–L10, 2006. doi:10.1152/ajplung.00135.2005.

28. **Mannock DA, McIntosh TJ, Jiang X, Covey DF, McElhaney RN.** Effects of natural and enantiomeric cholesterol on the thermotropic phase behavior and structure of egg sphingomyelin bilayer membranes. *Biophys J* 84: 1038–1046, 2003. doi:10.1016/S0006-3495(03)74920-0.

29. **Marrelli SP, Eckmann MS, Hunte MS.** Role of endothelial intermediate conductance KCa channels in cerebral EDHF-mediated dilations. *Am J Physiol Heart Circ Physiol* 285: H1590–H1599, 2003. doi:10.1152/ajpheart.00376.2003.

30. **Mukodani J, Ishikawa Y, Fukuzaki H.** Effects of hypoxia on sterol synthesis, acyl-CoA:cholesterol acyltransferase activity, and efflux of cholesterol in cultured rabbit skin fibroblasts. *Arteriosclerosis* 10: 106–110, 1990. doi:10.1161/01.ATV.10.1.106.

31. **Murata T, Lin MI, Stan RV, Bauer PM, Yu J, Sessa WC.** Genetic evidence supporting caveolae microdomain regulation of calcium entry in endothelial cells. *J Biol Chem* 282: 16631–16643, 2007. doi:10.1074/jbc.M607948200.

32. **Murata T, Sato K, Hori M, Ozaki H, Karaki H.** Decreased endothelial nitric-oxide synthase (eNOS) activity resulting from abnormal interaction between eNOS and its regulatory proteins in hypoxia-induced pulmonary hypertension. *J Biol Chem* 277: 44085–44092, 2002. doi:10.1074/jbc.M205934200.

33. **Murphy RC, Johnson KM.** Cholesterol, reactive oxygen species, and the formation of biologically active mediators. *J Biol Chem* 283: 15521–15525, 2008. doi:10.1074/jbc.R700049200.

34. **Nakane M, Mitchell J, Förstermann U, Murad F.** Phosphorylation by calcium calmodulin-dependent protein kinase II and protein kinase C modulates the activity of nitric oxide synthase. *Biochem Biophys Res Commun* 180: 1396–1402, 1991. doi:10.1016/S0006-291X(05)81351-8.

35. **Nguyen AD, McDonald JG, Bruick RK, DeBose-Boyd RA.** Hypoxia stimulates degradation of 3-hydroxy-3-methylglutaryl-coenzyme A reductase through accumulation of lanosterol and hypoxia-inducible factor-mediated induction of insigs. *J Biol Chem* 282: 27436–27446, 2007. doi:10.1074/jbc.M704976200.

36. **Norman AW, Demel RA, De Kruyff B, Van Deenen LL.** Substances of low molecular weight: studies on the biological properties of polyene antibiotics: evidence for the direct interaction of filipin with cholesterol of polyene. *J Biol Chem* 47: 1918–1929, 1972.

37. **Paffett ML, Naik JS, Resta TC, Walker BR.** Reduced store-operated Ca^{2+} entry in pulmonary endothelial cells from chronically hypoxic rats.

Am J Physiol Lung Cell Mol Physiol 293: L1135–L1142, 2007. doi:10.1152/ajplung.00432.2006.

38. **Paffett ML, Naik JS, Riddle MA, Menicucci SD, Gonzales AJ, Resta TC, Walker BR.** Altered membrane lipid domains limit pulmonary endothelial calcium entry following chronic hypoxia. *Am J Physiol Heart Circ Physiol* 301: H1331–H1340, 2011. doi:10.1152/ajpheart.00980.2010.
39. **Paffett ML, Riddle MA, Kanagy NL, Resta TC, Walker BR.** Altered protein kinase C regulation of pulmonary endothelial store- and receptor-operated Ca^{2+} entry after chronic hypoxia. *J Pharmacol Exp Ther* 334: 753–760, 2010. doi:10.1124/jpet.110.165563.
40. **Parpal S, Karlsson M, Thorn H, Strålfors P.** Cholesterol depletion disrupts caveolae and insulin receptor signaling for metabolic control via insulin receptor substrate-1, but not for mitogen-activated protein kinase control. *J Biol Chem* 276: 9670–9678, 2001. doi:10.1074/jbc.M007454200.
41. **Pollock JS, Förstermann U, Mitchell JA, Warner TD, Schmidt HH, Nakane M, Murad F.** Purification and characterization of particulate endothelium-derived relaxing factor synthase from cultured and native bovine aortic endothelial cells. *Proc Natl Acad Sci USA* 88: 10480–10484, 1991. doi:10.1073/pnas.88.23.10480.
42. **Pörn MI, Slotte JP.** Localization of cholesterol in sphingomyelinase-treated fibroblasts. *Biochem J* 308: 269–274, 1995. doi:10.1042/bj3080269.
43. **Potocnik SJ, Jenkins N, Murphy TV, Hill MA.** Membrane cholesterol depletion with β-cyclodextrin impairs pressure-induced contraction and calcium signalling in isolated skeletal muscle arterioles. *J Vasc Res* 44: 292–302, 2007. doi:10.1159/000101451.
44. **Prendergast C, Quayle J, Burdyga T, Wray S.** Cholesterol depletion alters coronary artery myocyte Ca^{2+} signalling in a stimulus-specific manner. *Cell Calcium* 47: 84–91, 2010. doi:10.1016/j.ceca.2009.11.009.
45. **Putney JW Jr, Broad LM, Braun FJ, Lievremont JP, Bird GS.** Mechanisms of capacitative calcium entry. *J Cell Sci* 114: 2223–2229, 2001.
46. **Romanenko VG, Rothblat GH, Levitan I.** Modulation of endothelial inward-rectifier K+ current by optical isomers of cholesterol. *Biophys J* 83: 3211–3222, 2002. doi:10.1016/S0006-3495(02)75323-X.
47. **Romanenko VG, Rothblat GH, Levitan I.** Sensitivity of volume-regulated anion current to cholesterol structural analogues. *J Gen Physiol* 123: 77–87, 2004. doi:10.1085/jgp.200308882.
48. **Rosado JA, Sage SO.** Protein kinase C activates non-capacitative calcium entry in human platelets. *J Physiol* 529: 159–169, 2000. doi:10.1111/j.1469-7793.2000.00159.x.
49. **Rosenhouse-Dantsker A, Noskov S, Durdagi S, Logothetis DE, Levitan I.** Identification of novel cholesterol-binding regions in Kir2 channels. *J Biol Chem* 288: 31154–31164, 2013. doi:10.1074/jbc.M113.496117.
50. **Singh AK, McMillan J, Bukiya AN, Burton B, Parrill AL, Dopico AM.** Multiple cholesterol recognition/interaction amino acid consensus (CRAC) motifs in cytosolic C tail of Slo1 subunit determine cholesterol sensitivity of Ca^{2+}- and voltage-gated K^+ (BK) channels. *J Biol Chem* 287: 20509–20521, 2012. doi:10.1074/jbc.M112.356261.
51. **Sooksawate T, Simmonds MA.** Effects of membrane cholesterol on the sensitivity of the $GABA_A$ receptor to GABA in acutely dissociated rat hippocampal neurones. *Neuropharmacology* 40: 178–184, 2001. doi:10.1016/S0028-3908(00)00159-3.
52. **Tatur S, Groulx N, Orlov SN, Grygorczyk R.** Ca^{2+}-dependent ATP release from A549 cells involves synergistic autocrine stimulation by coreleased uridine nucleotides. *J Physiol* 584: 419–435, 2007. doi:10.1113/jphysiol.2007.133314.
53. **Toselli M, Biella G, Taglietti V, Cazzaniga E, Parenti M.** Caveolin-1 expression and membrane cholesterol content modulate N-type calcium channel activity in NG108-15 cells. *Biophys J* 89: 2443–2457, 2005. doi:10.1529/biophysj.105.065623.
54. **Tuder RM, Chacon M, Alger L, Wang J, Taraseviciene-Stewart L, Kasahara Y, Cool CD, Bishop AE, Geraci M, Semenza GL, Yacoub M, Polak JM, Voelkel NF.** Expression of angiogenesis-related molecules in plexiform lesions in severe pulmonary hypertension: evidence for a process of disordered angiogenesis. *J Pathol* 195: 367–374, 2001. doi:10.1002/path.953.
55. **Wu S, Haynes J Jr, Taylor JT, Obiako BO, Stubbs JR, Li M, Stevens T.** Cav3.1 (α1G) T-type Ca^{2+} channels mediate vaso-occlusion of sickled erythrocytes in lung microcirculation. *Circ Res* 93: 346–353, 2003. doi:10.1161/01.RES.0000087148.75363.8F.
56. **Xia F, Xie L, Mihic A, Gao X, Chen Y, Gaisano HY, Tsushima RG.** Inhibition of cholesterol biosynthesis impairs insulin secretion and voltage-gated calcium channel function in pancreatic β-cells. *Endocrinology* 149: 5136–5145, 2008. doi:10.1210/en.2008-0161.
57. **Xu X, London E.** The effect of sterol structure on membrane lipid domains reveals how cholesterol can induce lipid domain formation. *Biochemistry* 39: 843–849, 2000. doi:10.1021/bi992543v.
58. **Yamamoto K, Furuya K, Nakamura M, Kobatake E, Sokabe M, Ando J.** Visualization of flow-induced ATP release and triggering of Ca2+ waves at caveolae in vascular endothelial cells. *J Cell Sci* 124: 3477–3483, 2011. doi:10.1242/jcs.087221.
59. **Zidovetzki R, Levitan I.** Use of cyclodextrins to manipulate plasma membrane cholesterol content: Evidence, misconceptions and control strategies. *Biochim Biophys Acta* 1768: 1311–1324, 2007.